Journal of
Composites Science

MDPI

Article

Reliability-Based Optimization of the Semi-Circular Bending Test for Asphalt Mixtures Using Cumulative Variability Trajectories

Hind Fadhil Abbas [1], Hasanain Radhi Radeef [2,*], Salam Ridha Aletba [3] and Zaid Hazim Al-Saffar [4]

[1] Department of Structures and Water Resources Engineering, College of Engineering, University of Kufa, Najaf 31221, Iraq; hindf.amarh@uokufa.edu.iq
[2] Department of Civil Engineering, College of Engineering, University of Kufa, Najaf 31221, Iraq
[3] College of Engineering, Wasit University, Wasit 52011, Iraq; salam.ridha@uowasit.edu.iq
[4] Department of Building and Construction Engineering Technology, Technical Engineering College/Mosul, Northern Technical University, Mosul 41002, Iraq; zaid.alsaffar@ntu.edu.iq
* Correspondence: hasanainr.aldulaimi@uokufa.edu.iq

Abstract

The semi-circular bend (SCB) test is widely used to characterize asphalt mixture cracking resistance. However, the practical usefulness of the test depends on the reliability of the measured fracture parameters. This study investigates SCB testing from a reliability perspective, with the aim of identifying the specimen number required for dependable interpretation and the testing conditions that provide the most stable response. The analysis considered nominal maximum aggregate size, notch depth, binder type, aging condition, test temperature, and loading rate. Fracture energy, peak load, and flexibility index, together with their cumulative coefficients of variation, were tracked from $n = 3$ to $n = 6$, while six-specimen raw datasets were used for Weibull reliability analysis. The results show that notch depth had the clearest effect on response stabilization, with the 15 mm notch providing the most reliable configuration and reaching the adopted variability limits earlier than the other notch depths. The descriptive Weibull analysis further indicated that the SBS-modified mixture exhibited the highest fracture-energy consistency within the tested dataset, whereas long-term aging, testing at 0 °C, and loading at 50 mm/min were associated with the lowest fracture-energy consistency within the tested dataset. Overall, SCB interpretation should be guided by response reliability, not mean fracture parameters alone. On this basis, a reliability-based SCB framework is proposed to support more dependable mixture comparison and more rational specimen planning.

Keywords: SCB test; asphalt mixture; fracture energy; flexibility index; reliability; cumulative COV; sample size optimization; Weibull analysis

Check for updates

Academic Editor: Luigi Solazzi

Received: 14 April 2026
Revised: 8 May 2026
Accepted: 10 May 2026
Published: 13 May 2026

Copyright: © 2026 by the authors. Licensee MDPI, Basel, Switzerland. This article is an open access article distributed under the terms and conditions of the Creative Commons Attribution (CC BY) license.

1. Introduction

Cracking remains one of the major distress mechanisms in asphalt pavements because it accelerates stages of structural deterioration [1]. By the time the cracking develops, water infiltrates throughout the mixture and causes oxidation, stripping, and progressive damage under traffic loading [2]. Therefore, the cracking resistance of asphalt mixtures is essential for pavement durability, life-cycle performance, and rational mix design. The fracture response of asphalt mixtures is integrally complicated because it is depend on the viscoelastic binder behavior, aggregate structure, air void distribution, temperature, loading rate, and aging state [3,4].

Several laboratory fracture tests were developed to evaluate the cracking resistance of asphalt mixture under controlled conditions [5,6]. Among these methods, the semi-circular bend (SCB) test has received sustained attention because it is relatively simple to prepare, easy to instrument, and capable of providing meaningful fracture parameters. The SCB configuration reproduces tensile stress concentration at the notch tip and provides a practical framework for studying crack initiation and propagation in asphalt mixtures [7,8]. These practical advantages explain why the SCB test has become common in research programs and increasingly relevant in performance-oriented specification frameworks.

A further advantage of the SCB method is that load–displacement curve can be used to derive several fracture parameters with different physical meanings [9,10]. Peak load reflects resistance to crack initiation, fracture energy represents the energy required for crack propagation through the remaining ligament, and the flexibility index captures the character of the post-peak softening response [11,12]. Together, these measures describe the capacity of the mixture to resist crack initiation and propagation by dissipating energy before and after crack growth [13]. This distinction is important because mixtures with similar peak loads can still behave very differently once fracture begins.

At the same time, recent studies outputs stated that SCB is sensitive to the test and material parameters during test implementation [3,14]. Results of fracture energy and related indices can be noticeably affected by specimen size, notch depth, loading rate, and temperature [15]. Such sensitivity means that the reliability of the test must be understood alongside the magnitude of the measured fracture parameters. A large average value has limited practical meaning if it is accompanied by high scatter or poor repeatability [16].

Mixture-related variables are equally influential. Aggregate skeleton structure controls crack tortuosity and aggregate interlock, and therefore affects how much energy must be dissipated as a crack propagates [17]. Moreover, studies have revealed that binder modification can change elastic behavior and stress redistribution capacity, while aging alters the balance between strength and brittleness by increasing oxidation and reducing ductility [18]. In addition, specimen conditioning and test temperature directly control the viscoelastic state of the asphalt matrix, thereby influencing both fracture resistance and plastic deformation [19]. As a result, SCB reliability should be interpreted as a combined outcome of material composition, conditioning history, and testing protocol rather than as a fixed attribute of the test method [20–22].

Although many published studies have examined how individual factors affect SCB fracture parameters, fewer studies have framed the method as a reliability and laboratory-design problem in which material composition, conditioning state, test protocol, and the required number of replicates are interpreted together [23–25]. That distinction is important because a mixture may perform superior on the basis of outcome results while still demanding additional replication under certain test conditions. The essential gap addressed in this study is therefore not the effect of a single variable on cracking resistance, but the lack of an integrated framework that connects factor sensitivity with practical replicate-number planning for dependable SCB implementation. Accordingly, the working hypothesis of this study is that SCB repeatability can be improved substantially when the required number of replicates is determined in relation to mixture condition and test configuration. To examine this hypothesis, the study combines COV analysis, Weibull analysis, and specimen-number optimization so that fracture response, factor effects, reliability, and replication demand can be interpreted together rather than separately. This study quantifies how NMAS, notch depth, aging, SBS modification, temperature, and loading rate affect the response of SCB fracture, identifies the testing conditions that provide the most stable and decision-relevant characterization of cracking resistance, and proposes condition-dependent guidance for the minimum number of replicates required for reliable SCB interpretation.

2. Materials and Methods

2.1. Materials

The materials used in this work were chosen to represent the asphalt mixtures typically adopted in Iraqi road construction. The aggregate gradation, binder selection, and mixture design were based on the Iraqi General Specifications for Roads and Bridges, Section R9: Hot-Mix Asphalt Concrete Pavement, issued by the State Commission for Roads and Bridges, Iraq [26]. This specification provided the local framework for defining the aggregate quality, gradation envelope, and Marshall mix design procedure. The binder and aggregate properties, as well as Marshall stability and flow, were determined using the relevant ASTM and AASHTO standards. After mixture preparation, the fracture behavior was assessed through the SCB test under the prescribed laboratory conditions [27].

2.1.1. Binder Materials

Two binders were used in the present study: a conventional 40–50 penetration-grade asphalt binder and a styrene–butadiene–styrene (SBS)-modified binder, as listed in Table 1. The base binder was selected because it is representative of binders commonly used in Iraqi asphalt paving applications, thereby improving the practical relevance of the study. Using a locally binder also ensures that the reliability analysis remains directly related to field-applicable mixtures rather than laboratory-specific materials.

Table 1. Measured properties of conventional and SBS-modified binders.

Property	Test Method	Conventional Binder	SBS-Modified Binder
Specific gravity @25 °C	D-70	1.03	1.04
Penetration @25 °C, 0.1 mm 100 g, 5 s	D-5	42.6	36.0
Ductility @27 °C (cm)	D-70	158	150
Softening Point, Ring & ball, °C	D-36	54	65
Retained Penetration @25 °C, 0.1 mm 100 g, 5 s	D-5	65.2	61.5
Residue Ductility @25 °C, 50 mm/min	D-113	87	105
Rotational Viscosity @135 °C & 165 °C, cp	D4402	575 & 146	920 & 240

The SBS-modified binder was prepared by incorporating 4% SBS by weight of binder using high-shear mixing at 175 ± 5 °C for 90 min at approximately 4000 rpm. This preparation procedure was adopted to ensure adequate dispersion of the polymer phase within the asphalt binder and to minimize the possibility that the measured fracture trends would be influenced by incomplete blending or modifier segregation. The same base binder was used for both the conventional and SBS-modified mixtures so that the effect of polymer modification could be isolated more clearly in the subsequent fracture analysis [28].

2.1.2. Aggregates

Crushed limestone aggregates obtained from a local Iraqi quarry were used as the coarse and fine aggregate fractions. Limestone was selected because it is widely used in Iraqi asphalt paving practice and provides a practical combination of strength, durability, and compatibility with bituminous binders. The use of a commonly adopted

aggregate type also improves the applicability of the findings to regional pavement engineering conditions.

The measured aggregate properties are listed in Table 2. The relative density and water absorption of coarse and fine aggregates were determined in accordance with ASTM C127-25 and ASTM C128-25, respectively [29,30]. The Los Angeles abrasion loss and aggregate crushing value show that the selected aggregate has sufficient resistance to wear and crushing during mixing, compaction, and loading. The measured specific gravity and absorption values also confirm that the aggregate is suitable for asphalt mixture preparation. These properties are not only related to conventional material quality, but also have a direct role in the fracture response of the mixture. Strong and durable aggregate particles can maintain aggregate interlock during loading, while the particle shape and surface texture may control the crack path and the degree of interaction between the binder and aggregate. Therefore, variations in these aggregate characteristics can influence both the measured SCB fracture parameters and their repeatability.

Table 2. Physical properties of aggregates.

Test	Obtained Value	Specification
Coarse Aggregate		
Bulk-specific gravity	2.666	ASTM C127
Apparent-specific gravity	2.739	ASTM C128
Loss Angeles abrasion	23.6%	45% max
Water absorption	0.72%	1.13%
Soundness	3.1%	18% max
Deleterious materials	0.92	3% max
Crushed percentage	95%	90% min
Fine Aggregate		
Bulk-specific gravity	2.658	-----
Apparent-specific gravity	2.722	-----

2.1.3. Mineral Filler

Limestone dust passing the 0.075 mm sieve was used as mineral filler. The measured specific gravity of the filler was 2.70. In addition to satisfying gradation and volumetric requirements, the filler contributed to mastic cohesion and improved particle packing within the mixture. Its content was kept consistent across all mixtures so that changes in fracture behavior could be attributed more reliably to nominal maximum aggregate size (NMAS), binder type, aging condition, and testing parameters rather than to differences in filler composition or dosage.

2.2. Aggregate Gradation and Mixture Design

The aggregate gradations and Marshall mix design properties of the conventional and SBS-modified asphalt mixtures are presented in Figure 1 and Table 3, respectively. Three gradations were selected with nominal maximum aggregate sizes (NMAS) of 9.5, 12.5, and 19 mm in order to examine the influence of aggregate structure on fracture behavior and test reliability. The selected gradations were established within the framework of the Iraqi SCRB specifications for hot-mix asphalt concrete and were intended to represent practical asphalt mixtures used in pavement surface and binder applications.

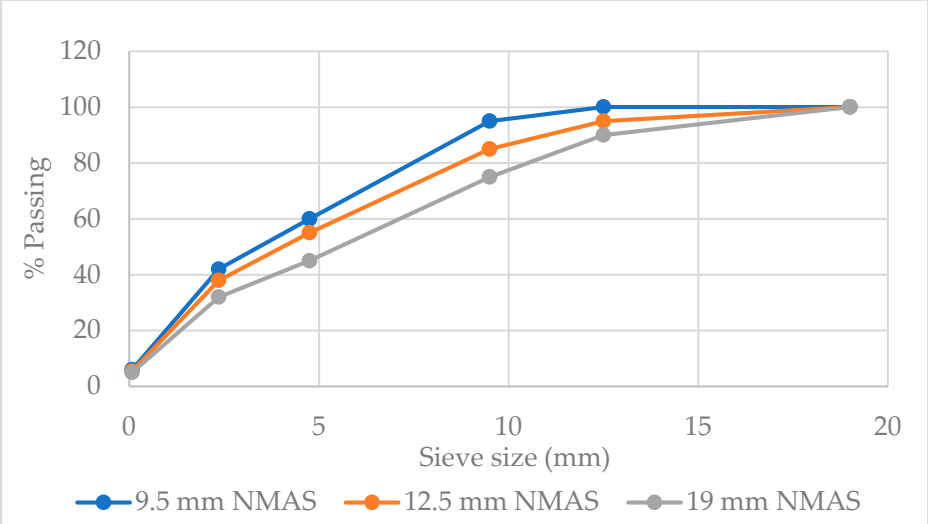


Figure 1. Aggregate gradation.

Table 3. Marshall mix design properties of the studied mixtures.

Mixture ID	Binder Type	NMAS (mm)	Optimum Asphalt Content (%)	Air Voids (%)	VMA (%)	VFA (%)	Marshall Stability (kN)	Flow (mm)
AC-9.5-C	Conventional	9.5	5.4	4.0	15.2	73.7	9.8	3.2
AC-9.5-SBS	SBS-modified	9.5	5.6	4.1	15.6	74.4	11.2	3.0
AC-12.5-C	Conventional	12.5	5.1	4.0	14.8	72.9	10.2	3.4
AC-12.5-SBS	SBS-modified	12.5	5.3	4.5	15.1	73.5	11.8	3.2
AC-19-C	Conventional	19	4.8	4.0	14.3	72.1	10.5	3.6
AC-19-SBS	SBS-modified	19	5.0	4.6	14.7	72.8	12.1	3.3

Mixtures were designed using the Marshall method to determine the optimum asphalt content. However, specimen compaction for SCB testing was performed using the Superpave gyratory compactor (CONTROLS S.p.A., Liscate, Italy) to well simulate field compaction conditions and to ensure improved internal structure representation [18,31]. The conventional mixtures exhibited optimum asphalt contents ranging from 4.8% to 5.4%, whereas the SBS-modified mixtures required slightly higher asphalt contents, which is consistent with the increased viscosity and improved coating characteristics of polymer-modified binders. The Marshall design results further show that the SBS-modified mixtures exhibited higher stability values than the corresponding conventional mixtures, indicating improved mixture cohesion and resistance to deformation. At the same time, the flow values remained within acceptable limits for the selected asphalt concrete mixtures, indicating that the improved stability was not accompanied by undesirable brittleness at the design stage.

The VMA and VFA values of both conventional and SBS-modified mixtures remained within acceptable design ranges, which indicates that the differences observed later in SCB fracture performance are primarily associated with binder modification, aggregate skeleton structure, and test conditions rather than major volumetric imbalance. Accordingly, the Marshall mix design results confirm that all mixtures were suitable for subsequent SCB testing and reliability evaluation.

2.3. Specimen Preparation and Aging Conditioning

Cylindrical specimens were compacted using a gyratory compactor. The following compaction parameters were used: vertical pressure of 600 kPa, gyration angle of 1.25°, and gyration speed of 30 revolutions per minute. A total of 100 gyrations were applied to achieve target air void content of 7.0 ± 0.5% [32]. Specimen height after compaction was approximately 115 ± 2 mm, from which semi-circular specimens of thickness B = 50 mm were cut. The resulting semi-circular specimens had a radius R = 75 mm (half of the 150 mm diameter) and a thickness B = 50 mm (Figure 2). A centered notch was introduced along the flat face using a masonry saw. Three notch depths were considered: 10, 15, and 20 mm. These depths span a practical range of notch-to-radius ratios and were selected to examine how notch geometry changes the stability of crack initiation and the repeatability of fracture measurements. Care was taken during cutting and notching to minimize geometric irregularities that could increase result scatter.



(**a**) (**b**)

Figure 2. Preparation of SCB specimens: (**a**) compacted cylindrical specimens before cutting and notching; (**b**) semi-circular specimens after cutting and notch formation.

Two laboratory aging conditions were adopted to reflect different stages of asphalt mixture hardening. The loose mixtures were first subjected to short-term aging at 135 °C for 4 h in a forced-draft oven, representing the hardening associated with plant mixing, transportation, and construction. Long-term aging was then applied to the compacted specimens at 85 °C for 5 days to account for the oxidative changes that occur during pavement service. Considering both aging levels was necessary because the objective of this study was not only to assess changes in mean fracture resistance, but also to determine whether aging alters the consistency and reliability of the SCB response. [33].

2.4. SCB Testing Procedure

SCB samples were tested using a universal testing machine under displacement control as shown in Figure 3. The test configuration comprising two lower roller supports with a span of 120 mm and a centered loading roller at the top. This setup was selected to remain consistent with common SCB practice while allowing systematic comparison across temperatures, loading rates, notch depths, and conditioning states [3].



Figure 3. SCB configuration mounted in the universal testing machine.

Six SCB specimens were tested for each unique combination of mixture type, aging condition, temperature, loading rate, and notch depth. The effect of specimen number was examined through a cumulative analysis from $n = 3$ to $n = 6$, while the full dataset at $n = 6$ was used to perform the Weibull reliability analysis. Testing was carried out at 0, 15, and 25 °C under loading rates of 0.5, 5, and 50 mm/min. Prior to loading, all specimens were conditioned until the target temperature was reached through the specimen thickness. This step was necessary because SCB fracture response is highly temperature-dependent; therefore, any temperature gradient within the specimen may locally alter mixture stiffness, affect crack initiation and propagation, and increase the apparent variability of the fracture parameters.

2.5. Fracture Parameters

The SCB load–displacement curve was used to determine peak load, fracture energy, and flexibility index. These quantities were selected because, taken together, they provide a broader description of fracture response than any single parameter alone. In practical terms, they describe the onset of cracking, the energy required for crack advance, and the character of post-peak softening, which makes them particularly suitable for reliability-oriented interpretation [1,34,35].

Peak load (Pmax) is the maximum load carried by the specimen before unstable crack growth. It is primarily associated with resistance to crack initiation and is influenced by mixture stiffness, notch geometry, temperature, and aggregate structure. Although peak load is a useful and intuitive measure, it does not on its own describe how the specimen behaves after cracking begins, which is why it must be interpreted together with energy-based and ductility-related measures.

Fracture energy (Gf) expresses the total mechanical work required to propagate the crack through the remaining ligament area. It is obtained by integrating the load–displacement response up to complete fracture and normalizing the resulting work by the ligament area. In asphalt mixtures, this parameter is especially informative because it captures the combined contribution of crack deflection, aggregate interlock, binder deformation, and the development of the fracture process zone [9]. Fracture energy was calculated using Equation (1)

$$Gf = \frac{W_f}{A_{lig}} \quad (1)$$

where W_f is the work of fracture calculated using Equation (2) and Alig is the ligament area calculated using Equation (3).

$$W_f = \int P \, d\delta \quad (2)$$

$$A_{lig} = (R - a) \times B \quad (3)$$

where P is the applied load, δ is the load-point displacement, R is the specimen radius, a is the notch depth, and B is the specimen thickness. In this study, R = 75 mm and B = 50 mm were kept constant across all specimens. Higher fracture energy values indicate greater energy dissipation during crack propagation and therefore better cracking resistance.

Flexibility index (FI) was calculated to characterize the post-peak cracking response of SCB samples. It was obtained from the fracture energy and the absolute value of the post-peak slope at the inflection point, as defined in Equation (4). From a practical fracture perspective, FI reflects the post-peak behavior of the mixture by distinguishing brittle mixtures, which lose their load-carrying capacity rapidly, from more flexible mixtures that dissipate fracture energy through gradual softening. Because brittle and ductile mixtures can sometimes have comparable peak loads, FI provides an additional level of interpretation that is highly useful when discussing cracking tolerance and testing reliability [35].

$$FI = \frac{Gf}{|m|B} \quad (4)$$

where m is the post-peak slope at the inflection point. Mixtures with steep post-peak softening exhibit lower FI and more brittle behavior, whereas mixtures with gradual load reduction exhibit higher FI and better cracking tolerance.

2.6. Statistical Analysis

To complement the cumulative convergence data, a descriptive distributional assessment was conducted. Given the practical laboratory sample size (n = 6), a two-parameter maximum-likelihood Weibull fit was applied to the raw fracture energy replicates. In this context, the Weibull shape parameter (β) is not intended to define a population-level predictive distribution, but rather to serve as a rigorous descriptive index of replicate-level scatter to supplement the empirical COV trajectories. A total of six replicate specimens were tested per condition. The descriptive distributional assessment and Weibull analysis were conducted using the complete n = 6 dataset. It should be noted that the experimental programme was designed as a reliability-oriented single-factor framework rather than a complete factorial design. Therefore, the dataset is suitable for assessing factor-wise

repeatability, cumulative variability, and practical replicate-number demand, but it does not permit a full statistical quantification of higher-order interaction effects. Possible interactions among mixture composition, ageing, temperature, loading rate, and notch geometry are therefore discussed qualitatively.

2.7. Replicate-Number Optimization

The adopted thresholds (COV Gf $\leq$ 15%, COV peak load $\leq$ 15%, COV FI $\leq$ 20%) are based on three lines of evidence. Nsengiyumva et al. reported that SCB fracture energy COV values below 15% are achievable under recommended testing conditions using well-prepared specimens [36]. Moreover, Majidifard et al. observed that FI typically exhibits 5–10% higher variability than Gf because it incorporates post-peak slope measurements; therefore, a 20% threshold for FI is statistically equivalent to a 15% threshold for Gf when accounting for additional measurement uncertainty [34]. According to ASTM C670, a Coefficient of Variation (COV) of 15% is widely accepted as representing "good" repeatability for fracture-based asphalt tests [37]. These thresholds are used in this study as practical screening criteria, not as universal specification limits for SCB testing.

The proposed formulation was used because it connects the optimization of specimen number with the actual reduction in variability observed in the three SCB fracture parameters. Conditions that reach the adopted COV limits at a smaller n indicate a more stable fracture response and, therefore, provide a more reliable basis for comparison. However, when the COV remains above the selected limits even at n = 6, the response should be considered more sensitive to specimen-to-specimen variation, and additional replication or more conservative interpretation may be needed. These COV limits are used here only as practical decision criteria for this specific experimental program. They are not proposed as general specification limits for SCB testing and should not be interpreted as mandatory requirements for other laboratory studies. Different research aims, materials, or quality-assurance applications may require stricter variability limits.

3. Results and Discussion

3.1. Effect of NMAS on Fracture Parameters

The influence of Nominal Maximum Aggregate Size (NMAS) on fracture response and cumulative stability is presented in Figure 4. In general, increasing NMAS increased the mean Gf, peak load, and FI values. The 19.0 mm mixture provided the highest fracture energy at n = 6, with a value of 601.0 J/m^2. This result is reasonable because larger aggregate particles can improve aggregate interlock and force the crack to follow a more tortuous path, thereby increasing the energy needed for crack propagation [38]. However, the improvement in fracture resistance did not necessarily mean better repeatability. The 9.5 mm mixture showed the lowest variability in Gf, with a COV of 10.3% at n = 6, while the larger NMAS mixture was more sensitive to specimen-to-specimen variation. This can be attributed to the higher local heterogeneity produced by large particles near the notch tip and along the fracture path. Thus, within the present dataset, the 19.0 mm NMAS improved the magnitude of fracture resistance, whereas the 9.5 mm NMAS provided a m. From a reliability standpoint, the 9.5 mm and 12.5 mm mixtures satisfied the adopted variability targets by n = 4 and n = 5, respectively. This suggests that mixtures with larger NMAS values (>12.5) may require more cautious interpretation or additional replication when evaluated using the SCB configuration.

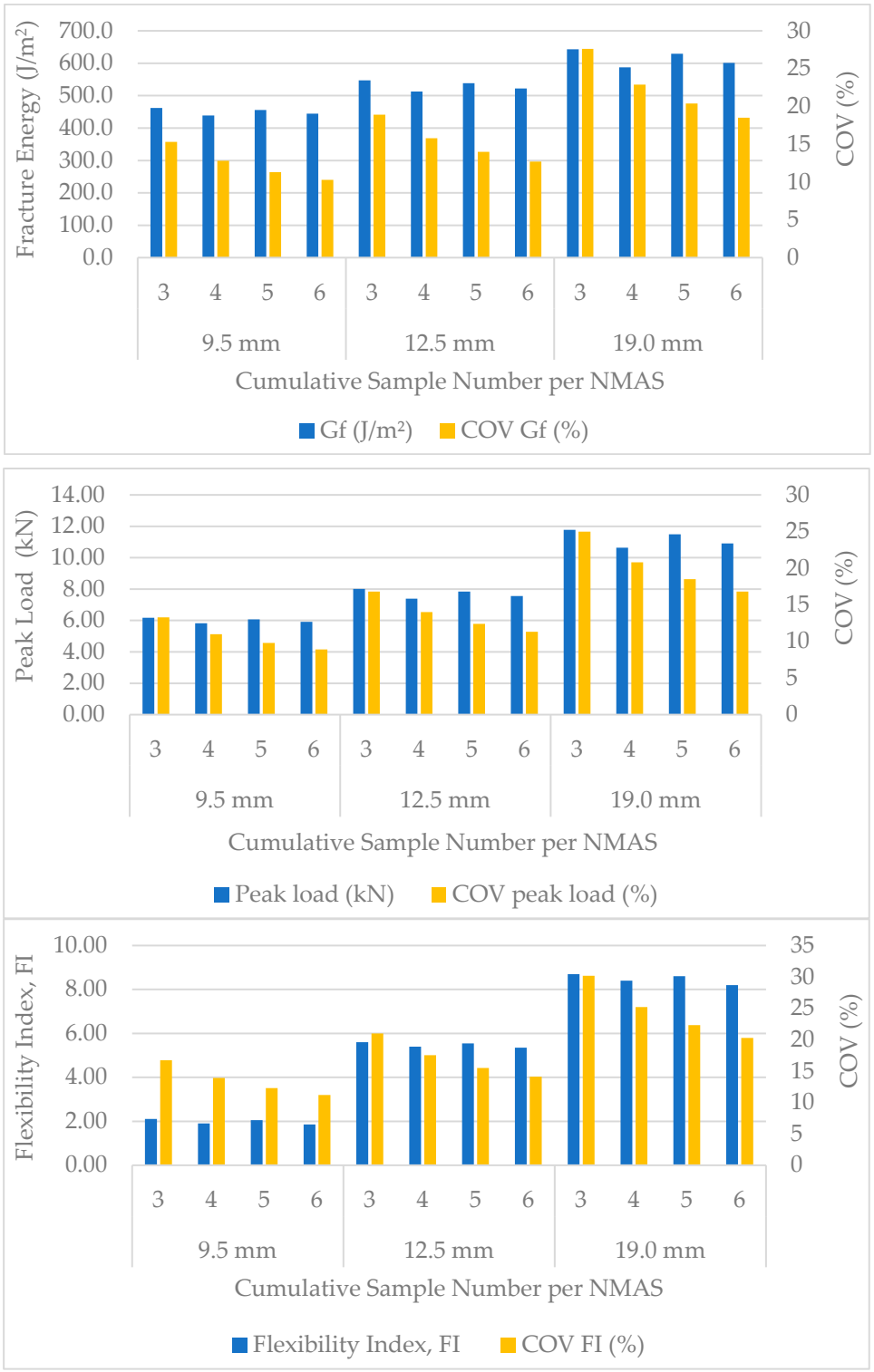


Figure 4. Effect of NMAS on cumulative fracture parameters and variability trajectories for n = 3 to n = 6.

3.2. *Effect of Notch Depth on Test Variability*

The effect of notch depth on the variability of the SCB fracture response is shown in Figure 5. Notch depth had the clearest influence on response stabilization among the examined testing variables. The cumulative variability trajectories showed that the 15 mm notch achieved the adopted reliability targets earlier than the 10 mm and 20 mm notches, indicating that it provided the most stable and efficient SCB configuration. Although the 10 mm notch produced relatively high fracture values, it required more specimens before

the response became sufficiently stable, while the 20 mm notch remained highly variable throughout the cumulative sequence. This behavior suggests that notch depth controls not only crack initiation severity, but also the repeatability with which fracture response can be measured. This study indicates that the 15 mm notch should be regarded as the most reliable notch configuration in the present study, because it provided the lowest cumulative variability. The results therefore support its use as the preferred notch depth for dependable SCB evaluation.

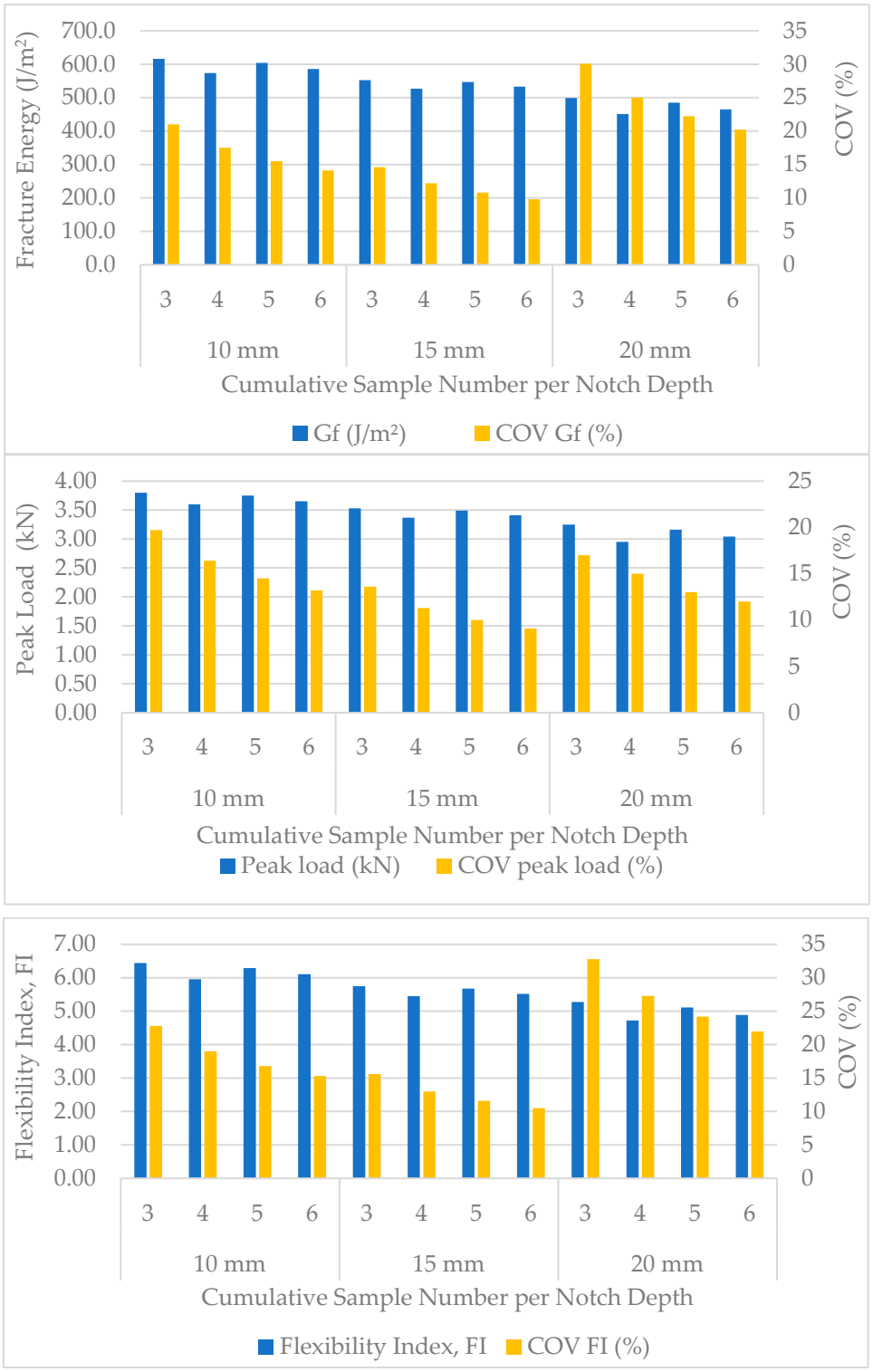


Figure 5. Effect of notch depth on cumulative fracture parameters and variability trajectories for $n = 3$ to $n = 6$.

Within the tested conditions, the 15 mm notch can be regarded as the most reliable notch configuration. This outcome is likely related to the role of ligament area in balancing notch-induced stress concentration and material representativeness. At this intermediate notch depth, the ligament remains sufficiently large to capture representative aggregate–binder interactions, while being adequately limited to localize the fracture process zone and minimize the influence of random microstructural heterogeneities. In contrast, the deeper notch depth of 20 mm significantly reduces the ligament area, making crack propagation more sensitive to local aggregate configuration in the vicinity of the notch tip. This enhances stochastic variability and results in less stable fracture behavior. Conversely, the 10 mm notch depth increased the ligament area and reduced the effective stress concentration at the notch tip. Under this condition, crack initiation may become less localized, allowing a wider deformation zone to develop before the main crack propagates. This can increase the contribution of local plastic deformation, particularly near the loading points, and may result in less uniform crack paths between specimens. Accordingly, a larger number of specimens may be required to obtain a stable statistical response. Overall, the 15 mm notch depth offered the most suitable compromise within the tested range, as it provided adequate crack localization while maintaining a representative ligament area. This led to better repeatability of the SCB parameters without losing the physical meaning of the fracture process.

3.3. Effect of Polymer Modification

As shown in Figure 6, SBS polymer modification noticeably influenced both the magnitude of the SCB fracture parameters and their statistical dispersion. At n = 6, the SBS-modified mixture recorded a mean Gf of 708.0 J/m^2, while the cumulative COV for Gf decreased from 15.2% (conventional binder) to 10.9%. From a testing reliability standpoint, this reduction in COV suggests that the viscoelastic state of the binder contributes to the repeatability of the SCB response. Conventional asphalt mixtures often exhibit a more brittle fracture response, making the crack initiation highly sensitive to the localized, heterogeneous structure at the notch tip such as the random orientation of aggregate edges or micro-voids. This high sensitivity to microscopic flaws naturally drives up replicate variability. In contrast, the elastomeric nature of SBS may improve mastic ductility and reduce the sensitivity of the fracture response to local structural variations. Consequently, the SBS-modified mixture showed a lower cumulative COV and a faster stabilization trend, indicating improved repeatability within the tested conditions. Consequently, the fracture response may become more consistent across replicate specimen, which mathematically manifests as a decreased COV and a faster stabilization rate for the test data.

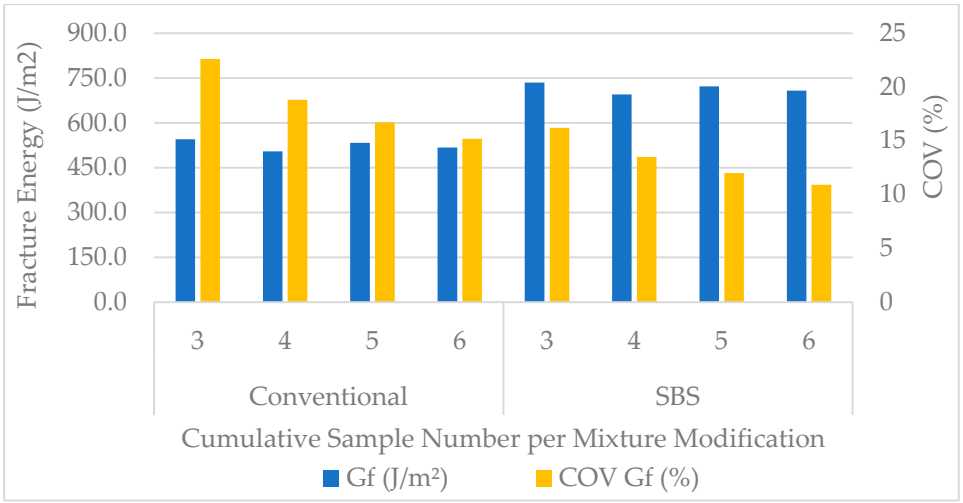


Figure 6. *Cont.*

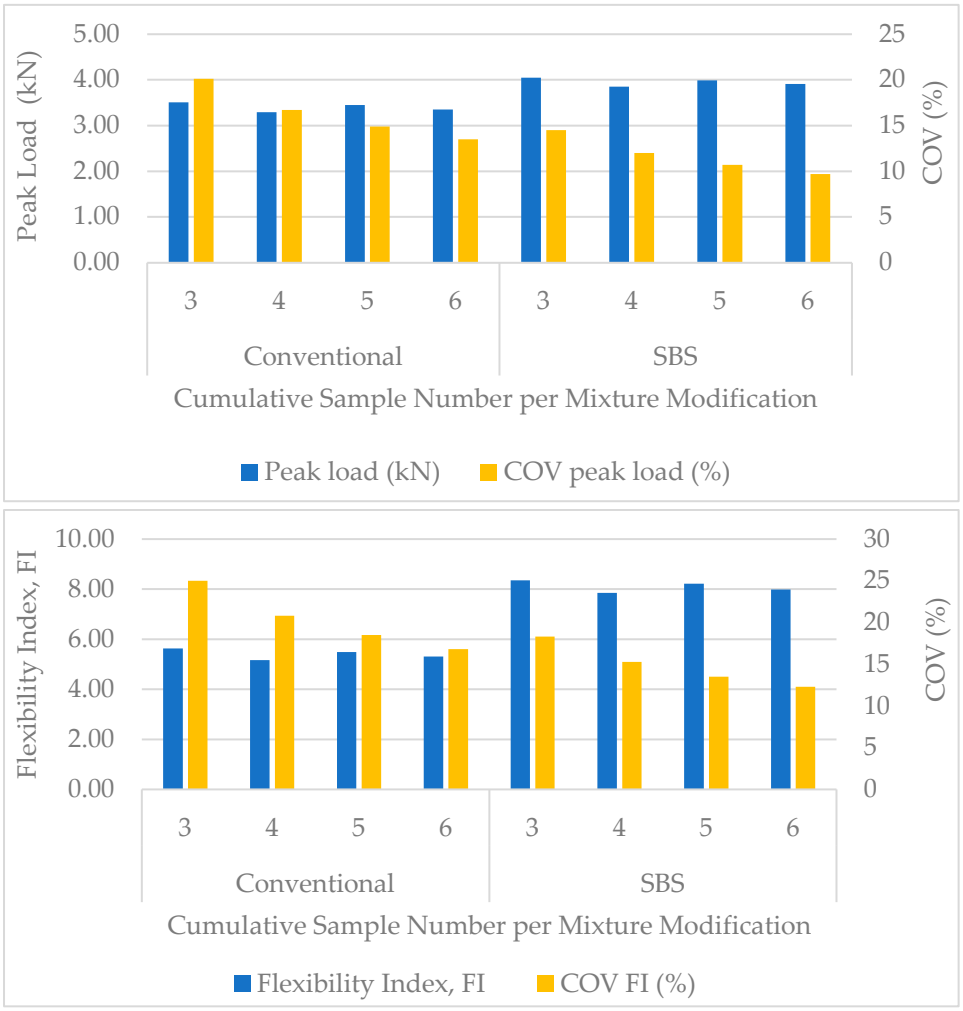


Figure 6. Effect of polymer modification on cumulative fracture parameters and variability trajectories for $n = 3$ to $n = 6$.

3.4. Effect of Aging

The effect of aging is presented in Figure 7. Increasing aging severity reduced both Gf and FI, whereas long-term aging increased peak load relative to the unaged and short-term aged conditions. At $n = 6$, the unaged mixture exhibited the highest mean Gf (625.0 J/m^2) and FI (6.45), while the long-term aged mixture showed the lowest Gf (435.0 J/m^2) and FI (3.25), together with the highest cumulative COV values (20.4% for Gf and 25.2% for FI). This trend is consistent with previous studies showing that oxidative aging increases stiffness and brittleness, thereby reducing cracking tolerance and fracture-related indices in asphalt mixtures [8,39]. The cumulative variability trajectories further indicate that none of the aging conditions satisfied all adopted stability targets by $n = 6$. Even the unaged and short-term aged states remained above the Gf or FI thresholds, whereas long-term aging was clearly the least stable condition. This suggests that aging affects not only the magnitude of the fracture response, but also the reliability with which that response converges toward a stable estimate. Similar reductions in cracking tolerance and flexibility-related performance after long-term aging have also been reported using FI-based and fracture-based approaches [8,40]. These studies indicate that oxidative aging stiffens the asphalt matrix, suppresses post-peak deformation capacity, and promotes a more brittle fracture response, thereby lowering flexibility-related indices and fracture resistance. Accordingly, caution is required when SCB is applied after aging conditioning,

because the increased variability of the aged response may require a larger number of specimens to achieve stable and reliable fracture evaluation.

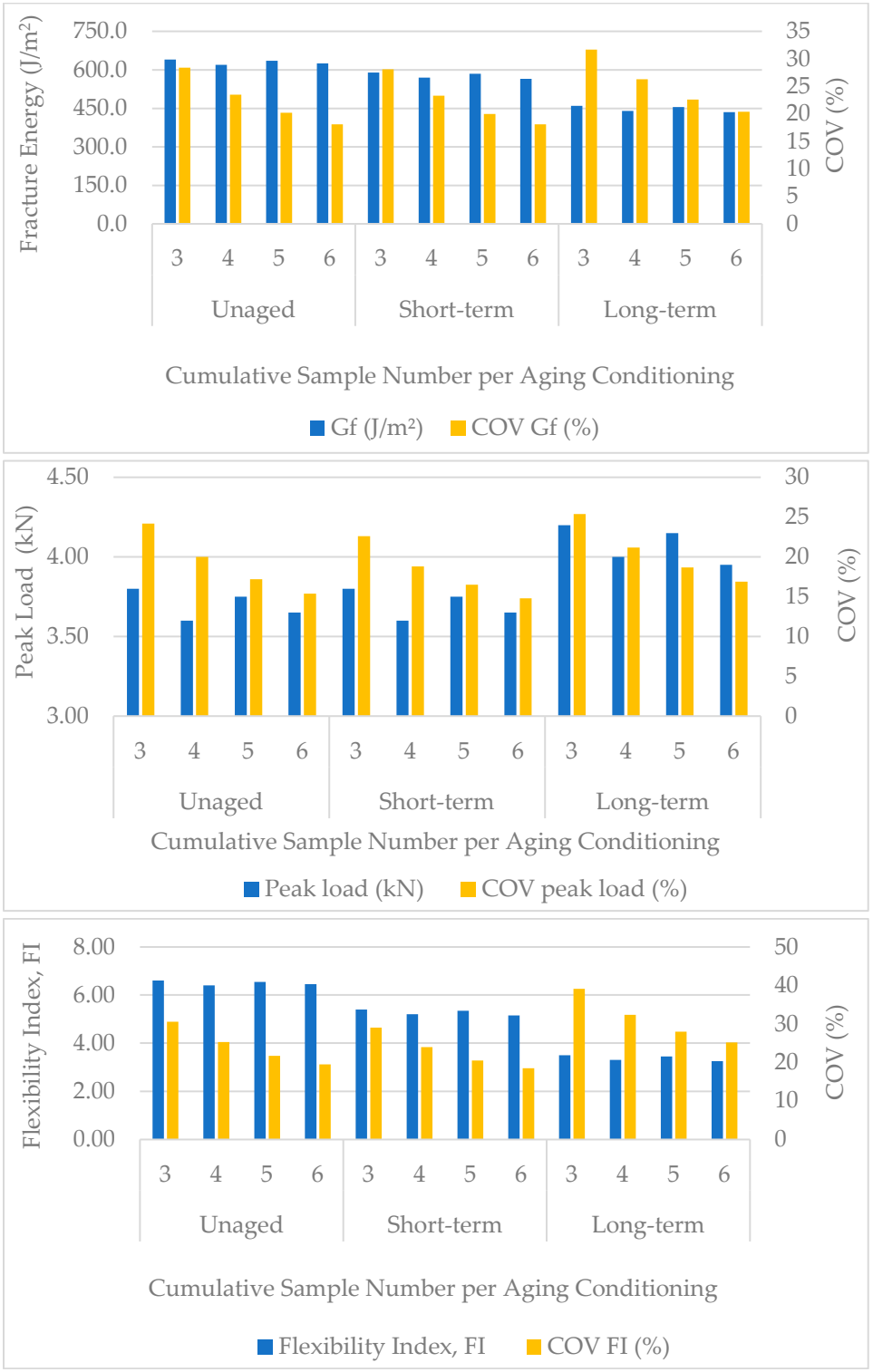


Figure 7. Effect of aging on cumulative fracture parameters and variability trajectories for $n = 3$ to $n = 6$.

3.5. Effect of Temperature

Temperature exerted a pronounced effect on the reliability of SCB interpretation, as presented in Figure 8. Among the examined temperatures, the 15 °C condition exhibited the lowest cumulative variability and the most stable convergence behavior, although it

still remained above at least one adopted threshold at $n = 6$. In contrast, the 0 °C and 25 °C conditions remained more variable throughout the cumulative sequence, indicating that both low- and high-temperature testing reduced the efficiency with which the SCB response stabilized as specimen number increased.

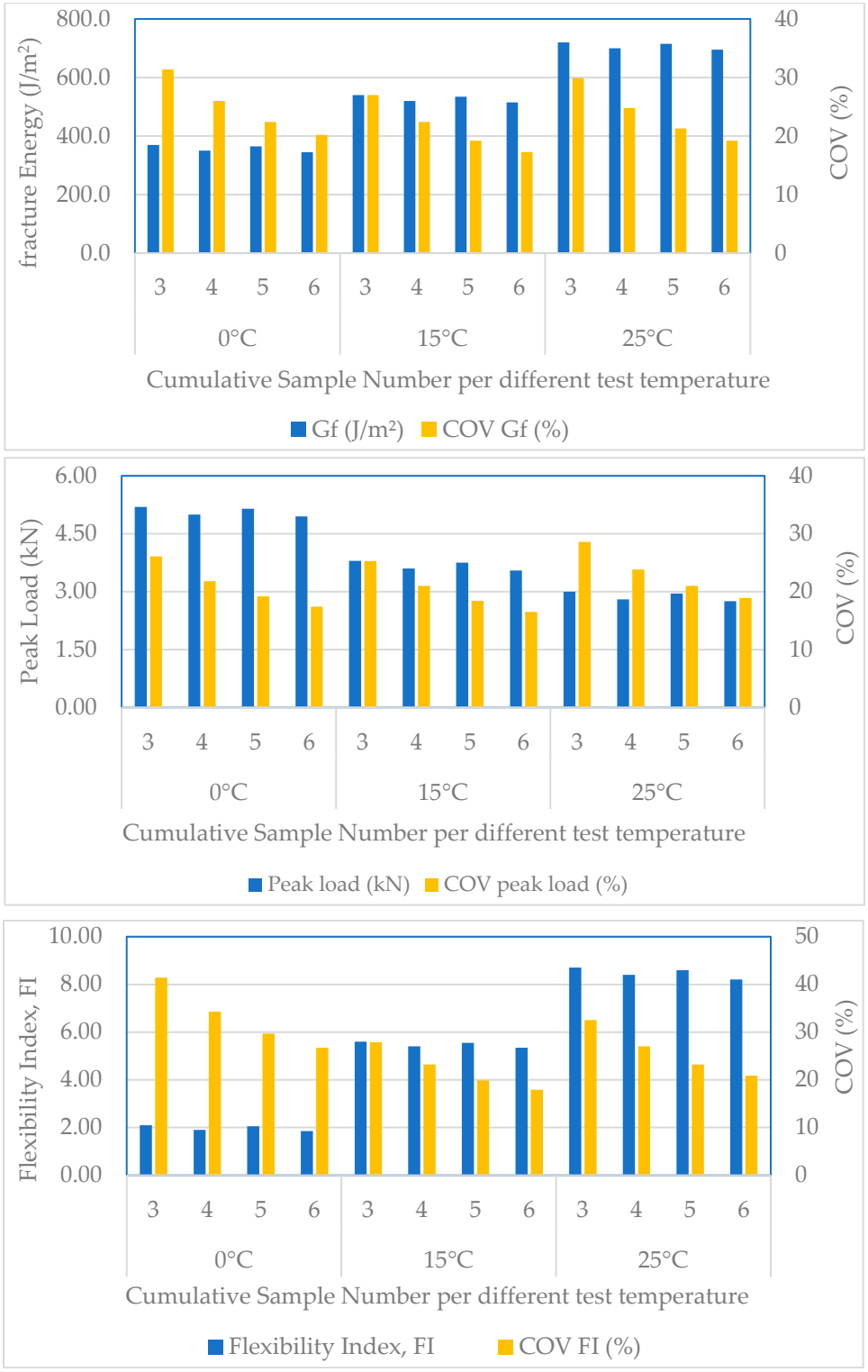


Figure 8. Effect of temperature on cumulative fracture parameters and variability trajectories for $n = 3$ to $n = 6$.

Mechanically, this behavior is consistent with the temperature-dependent viscoelastic nature of asphalt mixtures. At 0 °C, the mixture behaved in a stiffer and more brittle manner, which increased peak load but limited post-peak deformation and reduced both Gf and FI. At 25 °C, the mixture was able to dissipate more energy and sustain greater deformation after crack initiation, which increased Gf and FI, but the softer viscoelastic response also increased variability [41]. The 15 °C condition provided a more balanced fracture process in which crack initiation, energy dissipation, and post-peak softening developed in a more controlled manner, leading to lower cumulative variability than those observed at 0 °C and 25 °C.

Accordingly, the temperature results show that SCB evaluation should be based on response stability and replicate demand. Under the present testing range, 15 °C was the most balanced temperature condition, whereas 0 °C and 25 °C would require more cautious interpretation or additional specimens to achieve dependable SCB evaluation.

3.6. Effect of Loading Rate

Loading rate influenced both the SCB response and the stability of the measured results, as shown in Figure 9. Among the tested rates, 5 mm/min gave the most consistent behavior and the lowest cumulative variability, although at $n = 6$ it still remained slightly above one of the adopted stability limits. The rates of 0.5 and 50 mm/min showed greater variability throughout the cumulative sequence, which indicates that very slow and very fast loading make the SCB response less stable as the number of specimens increases.

This trend can be explained by the viscoelastic nature of asphalt mixtures. Under slow loading, the mixture has more time to deform, which tends to increase energy dissipation but also introduces more scatter in the response [42]. Under a higher loading rate, the mixture tends to behave in a more elastic and brittle manner, which may increase peak load while reducing the time available for viscous deformation and energy dissipation. At 5 mm/min, the fracture process developed in a more controlled way, giving a better balance between crack initiation, energy dissipation, and repeatability. These results indicate that loading rate should be selected primarily according to response stability rather than fracture magnitude alone. In the present study, 5 mm/min showed the most stable loading rate among the tested levels, whereas 0.5 and 50 mm/min would require more cautious interpretation or a larger number of specimens to achieve reliable SCB evaluation.

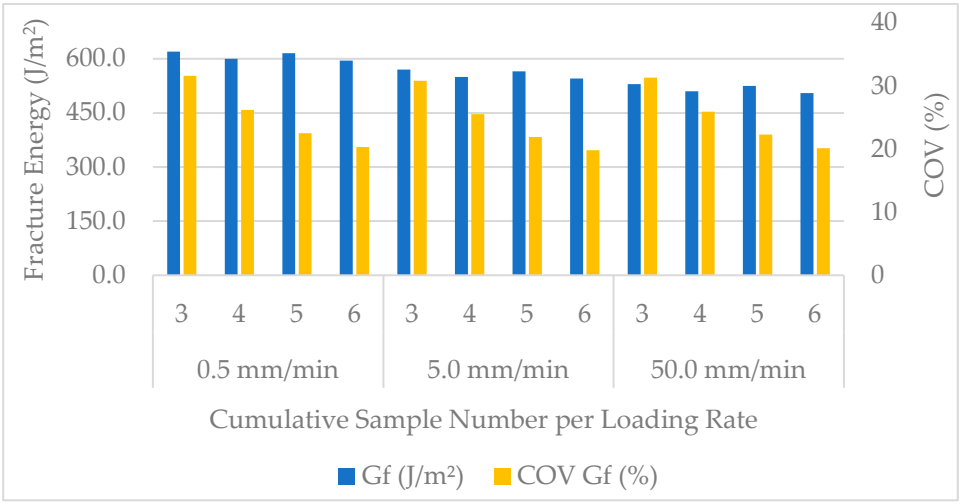


Figure 9. *Cont.*

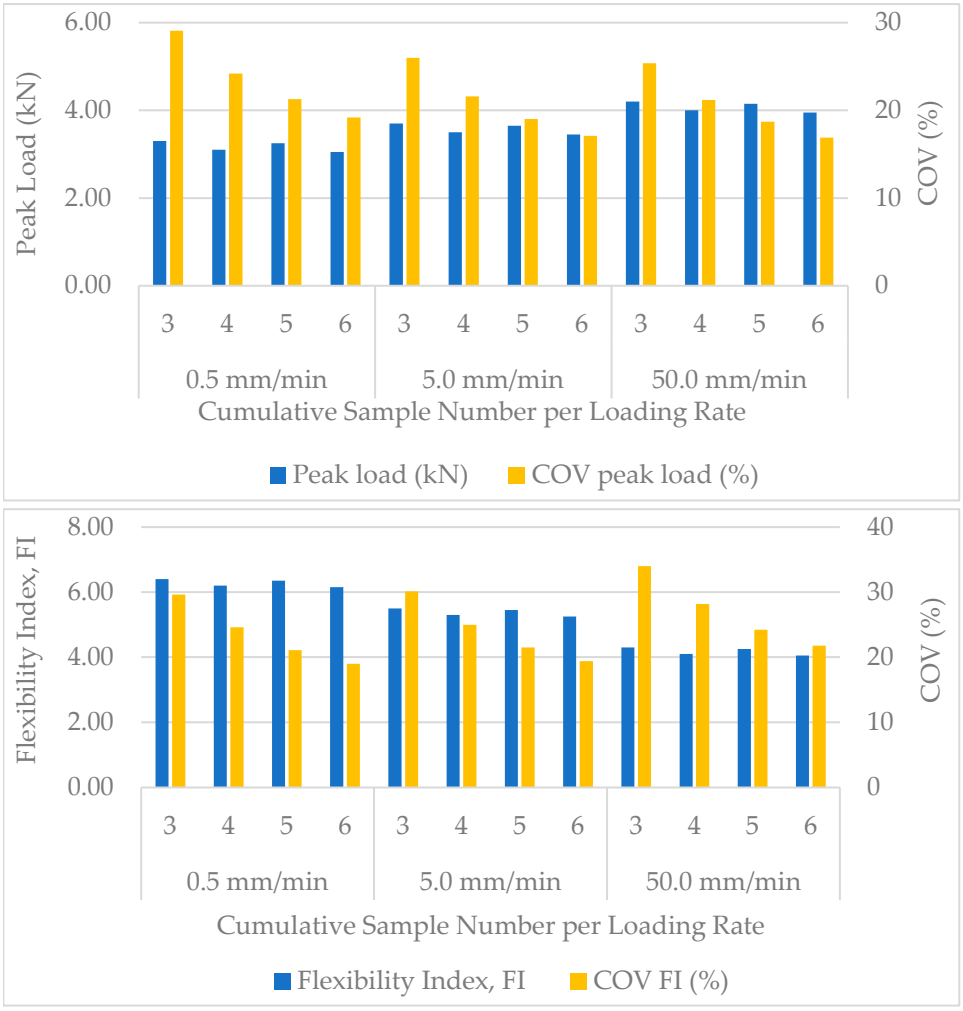


Figure 9. Effect of loading rate on cumulative fracture parameters and variability trajectories for $n = 3$ to $n = 6$.

3.7. Direct Weibull Reliability Analysis

The Weibull parameters summarized in Table 4 provide a descriptive comparison of fracture-energy variability across the investigated conditions rather than a definitive population-level reliability prediction. The shape parameter (β) shows clear sensitivity to mixture design and testing conditions, with higher values observed for NMAS 9.5 mm (β = 12.1), NMAS 12.5 mm (β = 9.8), and notch depth 15 mm (β = 12.6), indicating relatively lower scatter and more consistent crack propagation. Similarly, SBS-modified mixtures (β = 11.4) exhibit improved uniformity compared to conventional binders, supporting the stabilizing effect of polymer modification on fracture behavior. In contrast, lower β values associated with coarser NMAS (19 mm, β = 6.4), deep notch depth (20 mm, β = 5.7), and long-term aging (β = 5.6) reflect increased variability and a higher tendency toward brittle fracture. Environmental and loading conditions further influence variability, as evidenced by reduced β values under extreme temperatures (0 °C, β = 5.7) and non-optimal loading rates (0.5 and 50 mm/min, β ≈ 5.8), indicating unstable crack propagation under these conditions.

Table 4. Weibull parameters and reliability ranking for SCB fracture energy under different mixture and testing conditions.

Factor/Condition	Mean Gf (J/m^2)	COV Gf (%)	Scale η (J/m^2)	Shape β	Reliability Ranking
NMAS/9.5 mm	445.6	10.3	467.2	12.1	High
NMAS/12.5 mm	529.7	12.7	558.9	9.8	High
NMAS/19.0 mm	609.5	18.5	662.4	6.4	Moderate
Notch depth/10 mm	594.2	14.1	632.8	8.5	Moderate
Notch depth/15 mm	530.8	9.8	556.9	12.6	High
Notch depth/20 mm	465.5	20.2	511.9	5.7	Low
Binder/Conventional	519.5	15.2	556.4	7.6	Moderate
Binder/SBS	711.8	10.9	747.6	11.4	High
Aging/Unaged	620.0	18.1	674.2	6.5	Moderate
Aging/Short-term	581.7	18.1	632.2	6.5	Moderate
Aging/Long-term	450.0	20.4	495.6	5.6	Low
Temperature/0 °C	355.2	20.2	390.7	5.7	Low
Temperature/15 °C	529.0	17.3	571.9	6.9	Moderate
Temperature/25 °C	709.5	19.2	777.9	6.0	Moderate
Loading rate/0.5 mm/min	609.3	20.3	671.6	5.8	Low
Loading rate/5.0 mm/min	559.8	19.8	614.5	6.0	Moderate
Loading rate/50.0 mm/min	519.0	20.1	571	5.8	Low

However, it is important to emphasize that, due to the limited number of SCB replicates per condition, the Weibull parameters should be interpreted as indicative descriptors of relative variability rather than robust population-level reliability metrics. Accordingly, the assigned reliability rankings (high, moderate, low) reflect comparative consistency within the experimental dataset, and should not be directly extrapolated to field-scale failure probabilities. When considered alongside COV and ANOVA results, the Weibull analysis reinforces those intermediate conditions particularly NMAS 12.5 mm, notch depth 15 mm, SBS modification, and moderate loading/temperature conditions provide the most stable fracture response, while extreme conditions increase dispersion and uncertainty in measured performance.

Moreover, It should be noted that the Weibull analysis was applied only to Gf because fracture energy is the primary energy-based fracture parameter in the present study and is directly linked to crack-propagation resistance. Peak load and FI were evaluated through cumulative COV trajectories, which were used for replicate-number optimization. Therefore, the Weibull results should be interpreted as supplementary descriptors of Gf scatter rather than a complete distributional assessment of all SCB outputs.

3.8. Practical Implications and Optimisation of Replicate Number

From an implementation standpoint, the present results show that SCB testing should be interpreted as a cumulative-stability problem rather than as a single-point strength comparison. Figures 4–9 demonstrate that some conditions stabilize rapidly, while others remain highly variable even after six specimens. This means that a fixed replicate number may not be equally efficient across all material and testing conditions.

The threshold-based optimization in Table 5 shows that the 15 mm notch met the adopted targets by n = 3, the 9.5 mm NMAS mixture and SBS-modified binder by n = 4, the 12.5 mm NMAS mixture by n = 5, and the 10 mm notch by n = 6. In contrast, the 19.0 mm NMAS mixture, 20 mm notch, conventional binder, all aging states, all temperature states, and all loading-rate states remained above at least one adopted variability limit at n = 6. These results indicate that replicate planning should depend strongly on the expected variability regime of the test condition.

Table 5. Threshold-based recommended specimen number using COV Gf $\leq$ 15%, COV peak load $\leq$ 15%, and COV FI $\leq$ 20%.

Factor	Condition	Recommended n	Interpretation
NMAS	9.5 mm	4	First n meeting adopted variability targets
NMAS	12.5 mm	5	First n meeting adopted variability targets
NMAS	19.0 mm	>6	Threshold not reached by n = 6
Notch depth	10 mm	6	First n meeting adopted variability targets
Notch depth	15 mm	3	First n meeting adopted variability targets
Notch depth	20 mm	>6	Threshold not reached by n = 6
Binder type	Conventional	>6	Threshold not reached by n = 6
Binder type	SBS	4	First n meeting adopted variability targets
Aging	Unaged	>6	Threshold not reached by n = 6
Aging	Short-term	>6	Threshold not reached by n = 6
Aging	Long-term	>6	Threshold not reached by n = 6
Temperature	0 °C	>6	Threshold not reached by n = 6
Temperature	15 °C	>6	Threshold not reached by n = 6
Temperature	25 °C	>6	Threshold not reached by n = 6
Loading rate	0.5 mm/min	>6	Threshold not reached by n = 6
Loading rate	5.0 mm/min	>6	Threshold not reached by n = 6
Loading rate	50.0 mm/min	>6	Threshold not reached by n = 6

Accordingly, the practical novelty of this study lies in converting SCB reliability from a descriptive afterthought into an operational planning tool. The method does not merely compare means; it indicates how many specimens are needed before a given condition can be interpreted with reasonable confidence.

3.9. Study Limitations and Research Significance

The present study should be interpreted in light of the structure of the experimental dataset. The cumulative analysis provides a practical basis for replicate-number planning because it tracks how the mean response and COV evolve as the number of specimens increases from n = 3 to n = 6. However, the experimental program was not designed as a complete factorial matrix covering all possible combinations of mixture type, ageing condition, temperature, loading rate, NMAS, and notch depth. Therefore, the results are most suitable for factor-wise interpretation of SCB repeatability and practical specimen-number demand. Interaction effects among the investigated factors are discussed qualitatively, but they should be examined more rigorously in future studies using a full factorial design and a larger replicate population.

4. Conclusions

- Using the cumulative trajectories from $n = 3$ to $n = 6$, increasing NMAS increased mean Gf, peak load, and FI, but the lowest final cumulative variability within the NMAS set was obtained for the 9.5 mm mixture. The 19.0 mm mixture delivered the highest mean fracture response but did not satisfy the adopted variability limits by $n = 6$.
- Notch depth controlled both fracture level and stabilization rate. The 15 mm notch was the most stable and efficient configuration within the tested range meeting the adopted variability thresholds by $n = 3$, whereas the 20 mm notch remained highly variable at $n = 6$.
- SBS modification improved both fracture performance and measurement stability. Relative to the conventional binder, the SBS mixture increased final mean Gf from 517.0 to 708.0 J/m^2 and reduced final cumulative COV Gf from 15.2% to 10.9%.
- Aging degraded both mean fracture tolerance and reliability. Long-term aging produced the lowest final Gf (435.0 J/m^2) and FI (3.25), together with the highest cumulative variability among the aging conditions.
- Temperature strongly affected the measured fracture response. At 0 °C the mixtures showed the highest peak load but the lowest Gf and FI, while at 25 °C they showed the highest Gf and FI but still substantial cumulative variability. The 15 °C condition gave the most balanced response within the temperature set.
- Loading rate affected the balance between energy dissipation and brittle response, but none of the tested rates reached the adopted variability thresholds by $n = 6$. Thus, loading rate should be treated as a reliability-sensitive operating variable rather than a fixed default setting. Overall, the recommended specimen numbers are valid for the materials, specimen geometry, testing conditions, and COV limits adopted in this study, and should not be treated as universal SCB requirements.

Author Contributions: Conceptualization, H.R.R., H.F.A. and Z.H.A.; methodology, H.R.R. and H.F.A.; software, H.R.R.; validation, H.R.R. and Z.H.A.; formal analysis, H.F.A. and H.R.R.; investigation, H.F.A. and H.R.R.; resources, H.F.A. and Z.H.A.; data curation, H.R.R. and H.F.A.; writing—original draft preparation, H.R.R.; writing—review and editing, H.F.A. and Z.H.A.; visualization, H.R.R.; supervision, S.R.A. and Z.H.A.; project administration, S.R.A. and H.R.R. All authors have read and agreed to the published version of the manuscript.

Funding: This research received no external funding.

Data Availability Statement: The latest cumulative mean and cumulative COV worksheet used to update Figures 4–9 and Table 5, together with the revised manuscript file, are available from the corresponding author on reasonable request.

Acknowledgments: During the preparation of this manuscript, the authors used ChatGPT-4o (OpenAI) for assistance with English language editing, text refinement, and formatting. The authors reviewed, revised, and validated all content and take full responsibility for the final version of the manuscript.

Conflicts of Interest: The authors declare no conflicts of interest.

References

1. Radeef, H.R.; Abdul Hassan, N.; Mahmud, M.Z.H.; Zainal Abidin, A.R.; Ismail, C.R.; Abbas, H.F.; Al-Saffar, Z.H. Characterisation of cracking resistance in modified hot mix asphalt under repeated loading using digital image analysis. *Theor. Appl. Fract. Mech.* **2021**, *116*, 103130. [CrossRef]
2. Radeef, H.R.; Abdul Hassan, N.; Zainal Abidin, A.R.; Mahmud, M.Z.H.; Yaacob, H.; Mashros, N.; Mohamed, A. Effect of aging and moisture damage on the cracking resistance of rubberized asphalt mixture. *Mater. Today Proc.* **2021**, *42*, 2853–2858. [CrossRef]
3. Radeef, H.R.; Hassan, N.A.; Mahmud, M.Z.H.; Abidin, A.R.Z.; Jaya, R.P.; Ismail, C.R.; Abbas, H.F. Linear viscoelastic response of semi-circular asphalt sample based on digital image correlation and XFEM. *Measurement* **2022**, *192*, 110866. [CrossRef]

4. Chen, S.; Ge, D.; Jin, D.; Zhou, X.; Liu, C.; Lv, S.; You, Z. Investigation of hot mixture asphalt with high ground tire rubber content. *J. Clean. Prod.* **2020**, *277*, 124037. [CrossRef]
5. Ziari, H.; Moniri, A.; Bahri, P.; Saghafi, Y. The effect of rejuvenators on the aging resistance of recycled asphalt mixtures. *Constr. Build. Mater.* **2019**, *224*, 89–98. [CrossRef]
6. Wang, X.; Zhang, J.; Li, K.; Ding, Y.; Geng, L. Cracking Analysis of Asphalt Mixture Using Semi-circle Bending Method. *Iran. J. Sci. Technol. Trans. Civ. Eng.* **2021**, *45*, 269–279. [CrossRef]
7. Li, X.J.; Marasteanu, M.O. Using Semi Circular Bending Test to Evaluate Low Temperature Fracture Resistance for Asphalt Concrete. *Exp. Mech.* **2010**, *50*, 867–876. [CrossRef]
8. Radeef, H.R.; Hassan, N.A.; Mahmud, M.Z.H.; Usman, K.R.; Ismail, C.R.; Al Saffar, Z.H.; Abbas, H.F. Influence of ageing and moisture damage on the Illinois flexibility index value of polymer modified asphalt mixture. *Phys. Chem. Earth Parts A/B/C* **2022**, *128*, 103248. [CrossRef]
9. Yousefi, A.; Behnood, A.; Nowruzi, A.; Haghshenas, H. Performance evaluation of asphalt mixtures containing warm mix asphalt (WMA) additives and reclaimed asphalt pavement (RAP). *Constr. Build. Mater.* **2021**, *268*, 121200. [CrossRef]
10. Ince, R.; Yalcin, E.; Yilmaz, M. Quantifying nonlinear fracture parameters in bituminous SCB specimens: A compliance-based approach. *Case Stud. Constr. Mater.* **2024**, *21*, e03437. [CrossRef]
11. Golewski, G.L. Generalized fracture toughness and compressive strength of sustainable concrete including low calcium fly ash. *Materials* **2017**, *10*, 1393. [CrossRef]
12. Lu, D.X.; Bui, H.H.; Saleh, M. Effects of specimen size and loading conditions on the fracture behaviour of asphalt concretes in the SCB test. *Eng. Fract. Mech.* **2021**, *242*, 107452. [CrossRef]
13. Shi, X.; Mirsayar, M.M.; Mukhopadhyay, A.; Zollinger, D. Characterization of two-parameter fracture properties of portland cement concrete containing reclaimed asphalt pavement aggregates by semicircular bending specimens. *Cem. Concr. Compos.* **2019**, *95*, 56–69. [CrossRef]
14. Zhang, Y. Repeatability assessment of semi-circular bending test for asphalt mixtures: A inter-laboratory study. *Constr. Build. Mater.* **2024**, *412*, 134856.
15. Radeef, H.R.; Abdul Hassan, N.; Zainal Abidin, A.R.; Mahmud, M.Z.H.; Mohd Satar, M.K.I.; Mohd Warid, M.N.; Al Saffar, Z.H. Determining Fracture Energy in Asphalt Mixture: A Review. *IOP Conf. Ser. Earth Environ. Sci.* **2021**, *682*, 12069. [CrossRef]
16. Stewart, C.M.; Reyes, J.G.; Garcia, V.M. Comparison of fracture test standards for a super pave dense-graded hot mix asphalt. *Eng. Fract. Mech.* **2017**, *169*, 262–275. [CrossRef]
17. Christensen, C.O.; Schmidt, J.W.; Halding, P.S.; Kapoor, M.; Goltermann, P. Digital image correlation for evaluation of cracks in reinforced concrete bridge slabs. *Infrastructures* **2021**, *6*, 99. [CrossRef]
18. Radeef, H.R.; Hassan, N.A.; Katman, H.Y.; Mahmud, M.Z.H.; Abidin, A.R.Z.; Ismail, C.R. The mechanical response of dry-process polymer wastes modified asphalt under ageing and moisture damage. *Case Stud. Constr. Mater.* **2022**, *16*, e00913. [CrossRef]
19. Lastra-González, P.; Calzada-Pérez, M.A.; Castro-Fresno, D.; Vega-Zamanillo, Á.; Indacoechea-Vega, I. Comparative analysis of the performance of asphalt concretes modified by dry way with polymeric waste. *Constr. Build. Mater.* **2016**, *112*, 1133–1140. [CrossRef]
20. Pirmohammad, S.; Amani, B.; Shokorlou, Y.M.; Yousefi, A.A.; Sobhi, S.; Aliha, M.R.M.; Pirmohammad, S.; Haghshenas, H.F.; Ameri, M.; Abdipour, S.; et al. Laboratory investigations on fracture toughness of asphalt concretes reinforced with carbon and kenaf fibers. *Constr. Build. Mater.* **2020**, *226*, 106875. [CrossRef]
21. Vaseghi, Z.; Pirmohammad, S.; Momeni, R. Impact of SCB Specimen Size, Temperature, Loading Rate, and Loading Mode on Fracture Behavior of Asphalt Mixture Using Response Surface Method. *Fatigue Fract. Eng. Mater. Struct.* **2025**, *48*, 382–403. [CrossRef]
22. Kim, J. Reliability-based framework for fracture testing of asphalt materials. *Int. J. Pavement Eng.* **2025**, *26*, 245–267.
23. Ma, Y.; Mohammad, L.N.; Liu, J.; Asghar, M.; Elnaml, I.; Cooper, S.B., III; Cooper, S.B., Jr. Development of a cyclic semi-circular bending test protocol to characterize fatigue cracking of asphalt mixture at intermediate temperature. *Constr. Build. Mater.* **2024**, *443*, 137669. [CrossRef]
24. Chen, X. Interlaboratory repeatability of the semi-circular bend test for asphalt mixtures. *Road Mater. Pavement Des.* **2026**, *27*, 88–106.
25. Xing, C.; Han, Z.; Li, M.; Zhu, B.; Sun, Z.; Wang, Y.; Wang, S. Thermal history-induced nanoscale surface characteristics of bitumen: Implications of sample preparation on accurate characterization. *Appl. Surf. Sci.* **2026**, *730*, 166309. [CrossRef]
26. State Commission for Roads and Bridges. *General Specification for Roads and Bridges, Section R9: Hot-Mix Asphalt Concrete Pavement*, Revised ed.; Ministry of Housing and Construction: Baghdad, Iraq, 2003.
27. *Astm D6927-15*; Standard Test Method for Marshall Stability and Flow of Bituminous Mixtures. American Society for Testing and Materials: West Conshohocken, PA, USA, 2010.
28. Hossain, R.; Wasiuddin, N.M. Evaluation of Degradation of SBS Modified Asphalt Binder Because of RTFO, PAV, and UV Aging using a Novel Extensional Deformation Test. *Transp. Res. Rec.* **2019**, *2673*, 447–457. [CrossRef]

29. *Standard's ASTM C127-25*; Standard Test Method for Relative Density (Specific Gravity) and Absorption of Coarse Aggregate. ASTM International: West Conshohocken, PA, USA, 2025.
30. *Standard's ASTM C128-25*; Standard Test Method for Relative Density (Specific Gravity) and Absorption of Fine Aggregate. ASTM International: West Conshohocken, PA, USA, 2025.
31. *AASHTO R 30-24*; Standard Practice for Mixture Conditioning of Hot Mix Asphalt. American Association of State Highway and Transportation Officials (AASHTO): Washington, DC, USA, 2024.
32. *ASTM D8044-16*; Standard Method of Test for Evaluation of Asphalt Mixture Fracture Resistance Using the Semi-Circular Bend (SCB) Test at Intermediate Temperature. ASTM International: West Conshohocken, PA, USA, 2016.
33. *AASHTO R 30-02*; Standard Practice for Mixture Conditioning of Hot Mix Asphalt. American Association of State and Highway Transportation Officials: Washington, DC, USA, 2019.
34. Majidifard, H.; Jahangiri, B.; Rath, P.; Buttlar, W.G. Development of a balanced cracking index for asphalt mixtures tested in semi-circular bending with load-LLD measurements. *Meas. J. Int. Meas. Confed.* **2021**, *173*, 108658. [CrossRef]
35. Zarei, M.; Abdi Kordani, A.; Zahedi, M. Evaluation of fracture behavior of modified Warm Mix Asphalt (WMA) under modes I and II at low and intermediate temperatures. *Theor. Appl. Fract. Mech.* **2021**, *114*, 103015. [CrossRef]
36. Nsengiyumva, G.; You, T.; Kim, Y.R. Experimental-statistical investigation of testing variables of a semicircular bending (SCB) fracture test repeatability for bituminous mixtures. *J. Test. Eval.* **2017**, *45*, 1691–1701. [CrossRef]
37. *ASTM C670*; Standard Practice for Preparing Precision and Bias Statements for Test Methods for Construction Materials. ASTM International: West Conshohocken, PA, USA, 2023.
38. Alvergue, A.; Elseifi, M.; Mohammad, L.N.; Cooper, S.B. Laboratory evaluation of asphalt mixtures with reclaimed asphalt shingle prepared using the wet process. In *Proceedings of the Asphalt Paving Technology: Association of Asphalt Paving Technologists-Proceedings of the Technical Sessions, Atlanta, GA, USA, 16–19 March 2014*; DEStech Publications, Inc.: Lancaster, PA, USA, 2014; pp. 197–223.
39. Zhou, Z.; Gu, X.; Jiang, J.; Ni, F.; Jiang, Y. Fatigue cracking performance evaluation of laboratory-produced polymer modified asphalt mixture containing reclaimed asphalt pavement material. *Constr. Build. Mater.* **2019**, *216*, 379–389. [CrossRef]
40. Arabani, M.; Ferdowsi, B. Evaluating the Semi-Circular Bending Test for hma mixtures. *Int. J. Eng. Trans. A Basics* **2009**, *22*, 47–58.
41. Yousefi, A.A.; Sobhi, S.; Aliha, M.R.M.; Pirmohammad, S.; Haghshenas, H.F. Cracking Properties of Warm Mix Asphalts Containing Reclaimed Asphalt Pavement and Recycling Agents under Different Loading Modes. *Constr. Build. Mater.* **2021**, *300*, 124–130. [CrossRef]
42. Wang, H. Statistical variability in asphalt mixture fracture parameters: A meta-analysis. *Theor. Appl. Fract. Mech.* **2023**, *123*, 103712.

Disclaimer/Publisher's Note: The statements, opinions and data contained in all publications are solely those of the individual author(s) and contributor(s) and not of MDPI and/or the editor(s). MDPI and/or the editor(s) disclaim responsibility for any injury to people or property resulting from any ideas, methods, instructions or products referred to in the content.